Acoustic field in a thermoacoustic Stirling engine having a looped tube and resonator

doi: 10.1063/1.1533113

Acoustic field in a thermoacoustic Stirling engine having a looped tube and resonator

Yuki Ueda,[a] Tetsushi Biwa, and Uichiro Mizutani
Department of Crystalline Materials Science, Nagoya University, Nagoya 464, Japan

Taichi Yazaki
Department of Physics, Aichi University of Education, Kariya 448, Japan

(Received 26 August 2002; accepted 4 November 2002)

S. Backhaus and G. W. Swift [Nature **399**, 335(1999)] have built a prototype thermoacoustic Stirling engine based on traveling wave energy conversions, and demonstrated that its efficiency reached above 40% of the Carnot efficiency. We experimentally investigate an acoustic field in the engine through simultaneous measurements of velocity U and pressure P. By focusing on the phase lead Φ of U relative to P in its regenerator, we find that the engine can achieve such a high efficiency by the negative Φ about $-20°$ rather than a traveling wave phase ($\Phi=0$). © *2002 American Institute of Physics.* [DOI: 10.1063/1.1533113]

Mechanical parts such as pistons are indispensable for conventional heat engines to operate with a high efficiency. These parts result in high production and maintenance costs, and also require advanced technical skills about sliding seals.

More than 20 years ago, Ceperley showed a possibility to develop a class of heat engines without the nuisance moving parts.[1] He recognized that the gas in a traveling acoustic wave passing through a differentially heated regenerator undergoes a thermodynamic cycle similar to the Stirling cycle, and proposed a pistonless Stirling engine where traveling acoustic waves act as pistons of a conventional Stirling engine. This is because a phase lead Φ of cross-sectional mean velocity $U=ue^{i(\omega t+\Phi)}$ relative to pressure $P=pe^{i\omega t}$ in a traveling acoustic wave is the same as that within a regenerator of the conventional Stirling engine; ω is an angular frequency of the acoustic wave. Since the Stirling cycle is operated under thermodynamically reversible processes, the efficiency of the engine should ideally reach the Carnot efficiency.[2]

In 1998, Yazaki *et al.* first built the pistonless Stirling engine by using a thermoacoustic technique.[3] They experimentally observed that the energy conversion between heat flow Q and work flow I[4–7] is executed through the Stirling cycle in a looped tube engine by applying an experimental method of simultaneously measuring P and U.[3,8–11]

The next year, Backhaus and Swift demonstrated that the thermoacoustic Stirling engine had a high efficiency reaching 40% of the Carnot efficiency, or 30% of a thermal efficiency, by attaching a resonator to a looped tube engine.[12] On the basis of the simulation code *DeltaE* and equivalent electrical circuits, they reported that the phase lead Φ was a traveling wave phase ($\Phi=0$) and the dimensionless specific acoustic impedance[13] z contributing to the reduction of viscous losses reached 15–30 γ within the regenerator. Here z is defined as $z=(P/P_m)/(U/c)$, where P_m, c, and γ are a mean pressure, the adiabatic sound speed, and the specific heat ratio ($\sim$1.4 for air), respectively. They have attributed such a high efficiency to the phase ($\Phi=0$) and the large acoustic impedance. However, they have not experimentally measured the acoustic field in their engine.

In this letter, we reveal an acoustic field in a thermoacoustic engine having a looped tube and resonator by simultaneous measurements of P and U. The experimental results show that z is large enough to reduce viscous losses in the regenerator of the present engine. But the phase lead Φ in the regenerator is found to be negative instead of a traveling wave phase ($\Phi=0$). We will show below that the negative Φ plays a key role in producing the output power of the present engine. These results give the deeper understanding of thermoacoustics, and important information to develop the heat engines involving no moving parts.

The experimental apparatus is schematically illustrated in Fig. 1. The present thermoacoustic engine consists of a looped tube and resonator. Both the looped tube and resonator are made of Pyrex glass with an internal diameter of 40 mm. Total length of the looped tube is 1.18 m and that of the resonator is 1.04 m. One end of the resonator is connected to the 2.0×10^{-2} m^3 tank, and the other end to the looped tube. The looped tube has a 35 mm long regenerator consisting of a stack of 60-mesh stainless-steel screens with a wire diameter of 0.12 mm. The porosity of the regenerator is estimated

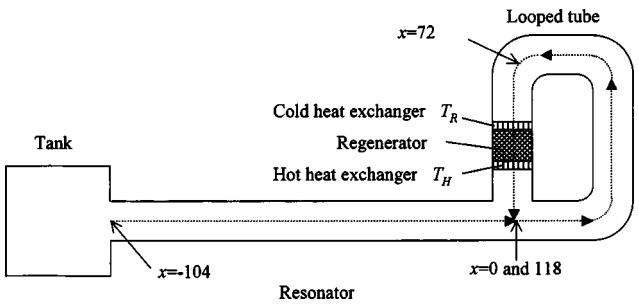

FIG. 1. The thermoacoustic Stirling engine consisting of a looped tube, resonator and tank. A joint position connecting the looped tube with the resonator is set to $x=0$ as an origin and the direction of x is taken anticlockwise in the looped tube and towards the right in the resonator, respectively.

[a]Electronic mail: ueda@mizu.xtal.nagoya-u.ac.jp

to be 0.82. The cold and hot heat exchangers are placed on both sides of the regenerator. An electrical heater is wound around the hot heat exchanger to control its temperature T_H, whereas the cold heat exchanger is kept at room temperature T_R ($\sim 18\,^\circ$C) by cooling water. Ducts of 10 mm length and 2 mm inner diameter are mounted on the looped tube and resonator walls, and are closed by pressure sensors. The present engine is filled with air at atmospheric pressure.

When T_H exceeds some critical value T_{cri}, the gas column spontaneously begins to oscillate with the frequency of 41 Hz. With this frequency, the oscillating gas can maintain good thermal contacts with the stainless-steel screens because the thermal penetration depth $\delta = 0.40$ mm[14] is larger than the hydraulic radius $r = 0.14$ mm[2,15] at the cold end of the regenerator. The temperature T_{cri} could be lowered by placing the hot end of the regenerator at the position close to the junction point ($x = 0$, 1.18 m). We revealed that the center of the regenerator should be located at $x = 0.9$ m to minimize T_{cri}. The value of T_{cri} under the condition above turned out to be 210 °C.

We simultaneously measured the pressure in the glass tube and the velocity along its central axis by the pressure sensor and laser Doppler velocimeter, respectively, while keeping $T_H = 278\,^\circ$C.[8,10] The pressure P is essentially independent of the radial coordinate in the glass tube because its radius is much smaller than the wavelength. On the other hand, the axial velocity possesses the radial distribution and thus the cross-sectional mean velocity U is determined from the measured velocity along the center axis by using the theoretical solution of the laminar flow (see Refs. 3 and 8 for more details).

The distributions of p, u, and Φ are shown in Figs. 2(a) and 2(b). The pressure amplitude p takes a minimum at $x = -1.04$ m and a maximum at $x = 0.85$ m. The distribution assures that the 1/4-wavelength acoustic oscillating mode is excited in this engine in the same way as Backhaus and Swift's.

Figure 2(c) shows the axial distribution of the work flow I determined by inserting the data shown in Figs. 2(a) and 2(b) into the definition

$$I = A\,\tfrac{1}{2} p u \cos\Phi, \tag{1}$$

where A is a cross-sectional area of the glass tube. The direction of I is represented by its sign. The work flow I fed back into the cold end of the regenerator ($x = 0.88$ m) is amplified from 1.7 to 2.2 W within the regenerator and the amplified work flow is output from the hot end ($x = 0.92$ m). This amplification of I running through the regenerator is caused by a characteristic traveling wave energy conversion process.[3,9,11] Therefore, the present engine works as a thermoacoustic Stirling engine. The difference of the work flow $\Delta I = 0.5$ W between the cold and hot ends of the regenerator represents the output power of the present engine, which compensates for energy dissipations in the resonator (0.1 W) and in looped tube (0.4 W).

Now we focus on the acoustic field near the regenerator responsible for the output power ΔI. The phase lead Φ gradually decreases there, and becomes a pure traveling wave phase at $x = 0.85$ m, close to the cold end of the regenerator. We found that p and u take maximum and minimum

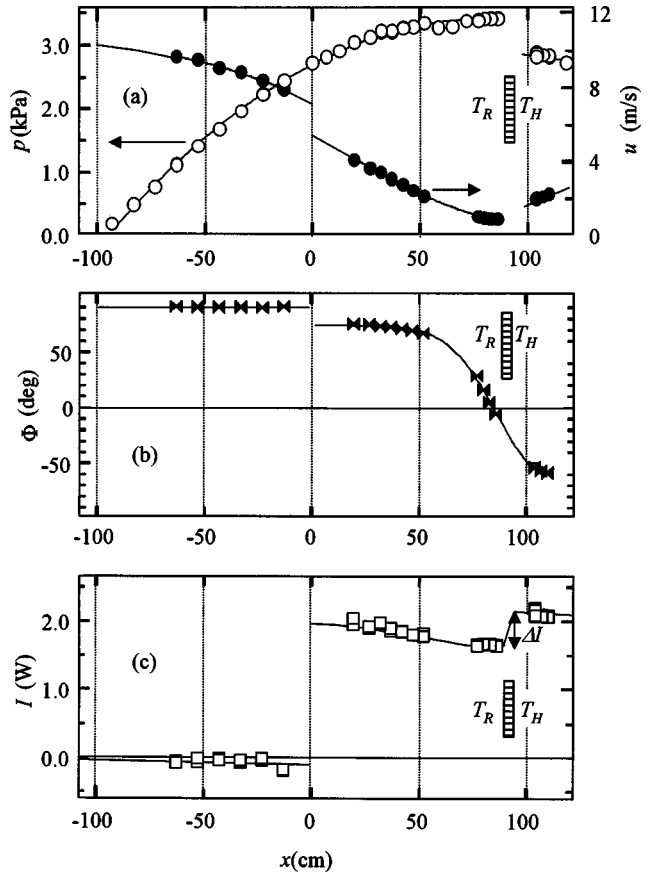

FIG. 2. Acoustic field in the looped tube ($0 \leqslant x \leqslant 118$) and the resonator ($-104 \leqslant x \leqslant 0$). (a) The axial distribution of $p(\bigcirc)$ and $u_m(\bullet)$. (b) The axial distribution of Φ. (c) The axial distribution of I. A shared area represents a regenerator and the lines are guides for the eye.

values at this particular position, respectively, and the dimensionless specific acoustic impedance z reaches ten times as large as γ near the regenerator. Therefore, the viscous losses in the regenerator can be well suppressed. Backhaus and Swift noted that a traveling wave phase should be formed in the regenerator.[12] However, we found Φ to be negative and about $-20°$ instead of $0°$ at the center of the present regenerator by interpolating from the both sides of the regenerator.

In order to see how a negative Φ contributes to the output power ΔI, we rewrite Eq. (1) as

$$\frac{\Delta I}{I} \simeq \frac{\Delta p}{p} + \frac{\Delta u}{u} - \tan\Phi \cdot \Delta\,\Phi, \tag{2}$$

where Δp, Δu, and $\Delta\,\Phi$ represent changes of p, u, and Φ at the hot end relative to those at the cold end, respectively. By inserting the experimental data shown in Fig. 2 into three terms on the right hand side of Eq. (2), we found that $\Delta p/p \sim -0.2$, $\Delta u/u \sim 0.7$, $-\tan\Phi \cdot \Delta\,\Phi \sim -0.2$ across the regenerator, resulting in $\Delta I/I \sim 0.3$. This shows that $\Delta I/I$ is mostly achieved through the second term. A positive and large contribution of the second term arises from the fact that the velocity node is located near the cold end of the regenerator. As a result, Φ inevitably becomes negative, because a velocity node is accompanied by a traveling phase ($\Phi = 0$) as we mentioned before. Though the negative Φ leads to negative values in the first and third terms, their contributions to $\Delta I/I$ are rather small relative to the second. If the regenerator was positioned at the velocity node where Φ is 0,

the second term would have also become small, as well as the first and third terms. Therefore, we consider that, in the present thermoacoustic Stirling engine, a negative Φ within the regenerator is essential for producing a large $\Delta I/I$ with reducing viscous losses in the regenerator.

Before ending, we try to estimate the efficiency of the thermoacoustic engine developed by Backhaus and Swift by using the present results, since they deduced it without a direct observation of ΔI. The work flow at the position, where a traveling wave phase ($\Phi=0$) is excited, is given by using Eq. (1) as

$$I=\frac{AP_mc}{2z}\left(\frac{p}{P_m}\right)^2, \tag{3}$$

where $\cos\Phi=1$ and $z=(p/P_m)/(u/c)$ are used. In their thermoacoustic engine, A is 6.2×10^{-3} m^2, P_m is 3 MPa and c is 1.0 km/s. They used a jet pump to suppress the dc flow, and thereby produced $p/P_m=0.1$ and $z=15-30$ γ ($\gamma\sim1.66$ for helium) with the input heat power of 4.0 kW. Hence, the work flow at the position, where $\Phi=0$ in their engine, would become 3.8-1.9 kW. Assuming that this amount of the work flow running into the regenerator is amplified by the ratio $\Delta I/I=0.3$ in the same way as that in the present engine, we can estimate the output power to be 1.1-0.6 kW. The value thus obtained would merely be referred to as a minimum output power for their engine, because the temperature ratio $\eta=(T_H-T_C)/T_C$ of 2.3 in their engine is higher than the present one ($\eta=0.8$). As a result, the thermal efficiency of their engine would become at least 25%-15%. This result demonstrates that a thermoacoustic Stirling engine having a looped tube and resonator can have a high efficiency, comparable to that of a conventional heat engine.

We built the thermoacoustic engine consisting of the looped tube and resonator, and revealed the acoustic field of the engine through the simultaneous measurements of pressure and cross-sectional mean velocity. By focusing on the acoustic field near the regenerator of the present engine, we showed how the thermoacoustic Stirling engine developed by Backhaus and Swift achieved a high efficiency through the creation of a negative Φ in a regenerator.

[1] P. H. Ceperley, J. Acoust. Soc. Am. **66**, 1508 (1979).
[2] G. W. Swift, D. L. Gardner, and S. Backgaus, J. Acoust. Soc. Am. **105**, 711 (1999).
[3] T. Yazaki, A. Iwata, T. Maekawa, and A. Tominaga, Phys. Rev. Lett. **81**, 3128 (1998).
[4] Work flow I is defined as $I=A\overline{PU}$, where the bar indicates the time average and A is cross-sectional area, and heat flow Q is defined as $Q=A\rho_m T_m\overline{\langle SU\rangle}$ where angular brackets represent radial average and ρ_m, T_m, S, and U are mean mass density, mean temperature, entropy per unit mass and axial velocity, respectively.
[5] A. Tominaga, Cryogenics **35**, 427 (1995).
[6] J. C. Wheatley, T. Hofler, G. W. Swift, and A. Migliore, Phys. Rev. Lett. **50**, 499 (1983); J. Acoust. Soc. Am. **74**, 153 (1983); Am. J. Phys. **53**, 147 (1988).
[7] G. W. Swift, Phys. Today **48**, 22 (1995); J. Acoust. Soc. Am. **84**, 1145 (1988).
[8] T. Yazaki and A. Tominaga, Proc. R. Soc. London, Ser. A **454**, 2113 (1998).
[9] T. Yazaki, T. Biwa, and A. Tominaga, Appl. Phys. Lett. **80**, 157 (2002).
[10] T. Biwa, Y. Ueda, T. Yazaki, and U. Mizutani, Cryogenics **41**, 305 (2001).
[11] Y. Ueda, T. Biwa, T. Yazaki, and U. Mizutani, in Proceedings of 17th International Congress on Acoustics, Rome, 2001; Part A.
[12] S. Backhaus and G. W. Swift, Nature (London) **339**, 335 (1999); J. Acoust. Soc. Am. **107**, 3148 (2000).
[13] If a freely traveling acoustic wave were used, the dimensionless specific acoustic impedance z would be fixed at γ.
[14] The thermal penetration depth δ is defined as $\sqrt{2\alpha/\omega}$, where α is a thermal diffusivity defined by using thermal conductivity κ, isobaric heat capacity per unit mass c_p, and mean density ρ_m as $\kappa/(c_p\rho_m)$.
[15] The hydraulic radius is defined as the ratio of gas volume to gas-solid wall contact surface area.